Development 128, 801-813 (2001)
Printed in Great Britain © The Company of Biologists Limited 2001
DEV7860

Transcriptional regulation of cytoskeletal functions and segmentation by a novel maternal pair-rule gene, *lilliputian*

Amy H. Tang[1,*], Thomas P. Neufeld[2], Gerald M. Rubin[1] and H.-Arno J. Müller[3,*]

[1]Howard Hughes Medical Institute, Department of Molecular and Cell Biology, University of California, Berkeley, Berkeley, California 94720-3200, USA
[2]University of Minnesota, Department of Genetics, Cell Biology and Development, Room 6-160 Jackson Hall, 321 Church Street S.E., Minneapolis, MN 55455, USA
[3]Institut für Genetik, Heinrich-Heine Universität Düsseldorf, Geb. 26.02., Universitätsstrasse 1, D-40225 Düsseldorf, Germany
*Authors for correspondence (e-mail: amy_tang@uclink4.berkeley.edu and muellear@uni-duesseldorf.de)

Accepted 21 December 2000; published on WWW 7 February 2001

SUMMARY

Transcriptional control during early *Drosophila* development is governed by maternal and zygotic factors. We have identified a novel maternal transcriptional regulator gene, *lilliputian* (*lilli*), which contains an HMG1 (AT-hook) motif and a domain with similarity to the human fragile X mental retardation FMR2 protein and the AF4 proto-oncoprotein. Embryos lacking maternal *lilli* expression show specific defects in the establishment of a functional cytoskeleton during cellularization, and exhibit a pair-rule segmentation phenotype. These mutant phenotypes correlate with markedly reduced expression of the early zygotic genes *serendipity α*, *fushi tarazu* and *huckebein*, which are essential for cellularization and embryonic patterning. In addition, loss of *lilli* in adult photoreceptor and bristle cells results in a significant decrease in cell size. Our results indicate that *lilli* represents a novel pair-rule gene that acts in cytoskeleton regulation, segmentation and morphogenesis.

Key words: *lilliputian* (*lilli*), Pair-rule gene, Cellularization, Actin cytoskeleton, Microtubule, *hkb*, *ftz*, *Sry α*, Lipid droplet transport, *Drosophila melanogaster*

INTRODUCTION

Development of many multicellular animals begins with the formation of an epithelium by cleavage divisions. Early development of *Drosophila* embryos is characterized by 13 rapid and synchronous mitotic division cycles that result in a syncytium containing 6000 nuclei at its cortical cytoplasm (Foe et al., 1993). A major developmental transition occurs during cycle 14 in which the syncytial blastoderm is converted into a blastoderm epithelium. This transition includes a variety of cellular events, such as contraction of an actin-myosin network, microtubule-driven transport of organelles, formation of cell membranes, and a marked increase in zygotic transcription (Schejter and Wieschaus, 1993a). This transitional event ultimately results in the formation of individual cells at the cortex and thus is called cellularization.

Formation of the blastoderm epithelium during cellularization is driven by a contractile actin-myosin network that forms between individual nuclei and proceeds along the leading edges of the advancing furrow membranes. The zygotically active genes *nullo*, *serendipity alpha* (*Sry α*), and *bottleneck* (*bnk*) are required to maintain this cytoskeletal network during cellularization (Merrill et al., 1988; Wieschaus and Sweeton, 1988). These genes encode novel membrane-associated proteins that regulate different aspects of actin dynamics and cytoskeleton organization. These molecules have been proposed to play a direct role in regulating the dynamic reorganization and interaction of the contractile actin-cytoskeleton with the newly forming plasma membranes of cellularizing embryos (Schweisguth et al., 1990; Simpson-Rose and Wieschaus, 1992; Schejter and Wieschaus, 1993b; Hunter and Wieschaus, 2000). The *nullo*, *Sry α*, and *bnk* genes are expressed in a similar spatiotemporal pattern, with onset of expression at nuclear cycle 11, peak expression at cycle 13/early cycle 14, and downregulation in late cycle 14 (Schweisguth et al., 1989; Simpson-Rose and Wieschaus, 1992; Schejter and Wieschaus, 1993a; Schejter and Wieschaus, 1993b). Although the factors that regulate expression of these blastoderm-specific transcripts are not known, genetic evidence suggests that the onset of expression of the *Sry α* and *nullo* genes might depend on maternal gene products rather than a unique zygotically active regulator (Merrill et al., 1988; Wieschaus and Sweeton, 1988; Simpson-Rose and Wieschaus, 1992; Ibnsouda et al., 1995).

The cytoskeletal network is also required during the syncytial blastoderm stage for the correct localization of certain segmentation gene products that provide a framework for patterning the embryo (Nüsslein-Volhard and Wieschaus, 1980; Davis and Ish-Horowicz, 1991). Specifically, the transcripts of the zygotic pair-rule genes *fushi tarazu* (*ftz*) and *hairy* (*h*) are localized exclusively to the apical periplasm by a selective vectorial export mechanism (Hafen et al., 1984;

Ingham et al., 1985; Davis and Ish-Horowicz, 1991; Lall et al., 1999). Pair-rule genes have been characterized by their mutant phenotypes demonstrating their requirement in the formation of alternate segments, by their expression pattern in seven stripes, and by their requirement in morphogenetic movements. Many zygotic pair-rule gene mutants exhibit defects in the extension of the germband during gastrulation (Irvine and Wieschaus, 1994). Germband extension represents the planar elongation and narrowing of the ectodermal cell layer during gastrulation (Costa et al., 1993). During this process the germband elongates twofold and narrows to about half its original width. Cell intercalation is observed during germband extension and has been proposed to be the driving force of the extension movements (Irvine and Wieschaus, 1994). Since all known pair-rule genes encode transcription factors, they cannot be the primary regulators of the extension movements.

Here we describe a novel pair-rule gene that is essential for proper cellularization, gastrulation and segmentation during embryogenesis. Since clonal analysis in the adult eye indicated that photoreceptor cells mutant for this gene are reduced in size (Neufeld et al., 1998b), we named this gene *lilliputian (lilli)*. Mutations in *lilli* have been identified in a number of independent genetic screens as dominant suppressors of transgene-dependent phenotypes in the adult *Drosophila* eye (Neufeld et al., 1998b; Rebay et al, 2000), and we provide evidence that this suppression reflects a requirement of *lilli* in the proper transcription of these transgenes. In addition, in germline clone (GLC) embryos lacking all *lilli* gene product, the expression of a number of zygotic regulators required for cellularization and early patterning are defective, including *Sry α*, *ftz* and *huckebein* (*hbz*). Our results suggest that *lilli* directs early developmental events, such as cellularization and patterning, through transcriptional activation of a specific group of zygotic regulators.

MATERIALS AND METHODS

Fly genetics and clonal analysis

Fly cultures and crosses were carried out according to standard procedures. Two *lilli* mutant alleles (*lilli*^{XS575} and *lilli*^{XS407}) were recombined onto a 2L-FRT chromosome, mitotic clones were generated as described previously (Xu and Rubin, 1993), and germline clones were generated as described previously (Chou and Perrimon, 1996). All mutant analyses were performed using these alleles unless otherwise indicated. FACS analysis and area measurements of *lilli* mutant clones were performed as described (Neufeld et al., 1998a; Zhang et al., 2000).

Molecular biology

Plasmid rescue was used to isolate genomic DNA adjacent to the P element *lilli*$^{l(2)00632}$. The genomic fragment was used as a probe to screen a *Drosophila* imaginal disc cDNA library (a gift from A. Cowman) and subsequently the *Drosophila* LP, GH and LD libraries (Rubin et al., 2000). One full-length *lilli* cDNA was isolated, sequenced and cloned into *pUAS* (Brand and Perrimon, 1993). Transgenic lines were established using P-element-mediated transformation and used in misexpression and rescue experiments. In addition, a large number of *lilli* cDNA species that may represent different splicing variants have been isolated. The full-length *lilli* cDNA isolated and characterized in this paper has the GenBank accession number AF289034.

CAT assay

Third instar wandering larvae were washed with phosphate-buffered saline, and resuspended in Passive Lysis Buffer (Promega). The chloramphenicol acetyltransferase (CAT) assays were performed in the linear range of the reaction on TLC plates as described previously (Courey and Tjian, 1988). Data from three to six experimental sets were quantitated on a Fuji phosphorimager and averaged.

Timelapse video recording, histology and immunofluorescence (IF) staining

For live observations and video timelapse analysis, the embryos were prepared as described by Wang et al. (Wang et al., 1999). For α-Nullo and α-Bnk double immunolabeling, embryos were heatfixed as described (Müller and Wieschaus, 1996). Immunohistochemical staining of embryos was performed as described (Müller et al., 1999). In situ hybridization to embryos and imaginal discs was carried out essentially as described by Tautz and Pfeifle (Tautz and Pfeifle, 1989). Scanning electron microscopy was performed as described by Kimmel et al. (Kimmel et al., 1990). Fixation, embedding and sectioning of adult eyes were performed as described previously (Wolff and Ready, 1991). Confocal microscopy was carried out using a Leica TCS-NT confocal microscope and images were processed with Adobe Photoshop 5.5 on a Macintosh computer.

Flow cytometry

lilli and *lilli-Pten* homozygous mutant clones induced by FLP/FRT-mediated recombination were marked by the absence of GFP expression using a ubiquitin-GFP FRT40A chromosome (kindly provided by Christina Martin-Castellanos). Fluorescence-activated cell sorting (FACS) of dissociated wing disc cells was carried out as previously described (Neufeld et al., 1998a).

RESULTS

Identification and characterization of *lilli* as a transcriptional regulator

Phyllopod (Phyl) is one of the most downstream nuclear components identified in the Sevenless receptor tyrosine kinase-RAS1 signaling pathway (Chang et al., 1995; Dickson et al., 1995). Using the eye-specific expression vector pGMR, which contains a multimerized binding site for the zinc-finger protein Glass placed upstream of the basal *hsp70* promoter (Hay et al., 1994), we expressed Phyl in all cells posterior to the morphogenetic furrow during larval development, and in all cells except cone cells in the pupal eye. This resulted in a rough eye phenotype that we used to screen for dominant modifiers. The *lilli* gene corresponds to one of the complementation groups that strongly suppress the rough eye phenotype of *GMR-phyl* (Fig. 1A,B). Complementation analyses revealed that many *lilli* alleles have been identified as suppressors in a number of different GMR-based dominant modifier screens. For example, *lilli* alleles were isolated in a *GMR-sina* screen (also called *SS2-1*; Neufeld et al., 1998b) and in a *GMR-Yan*^{ACT} screen (also called *SY2-1*; Rebay et al., 2000). Mutations in *lilli* suppress the rough eye phenotypes generated by overexpression of either positive (Sina and Phyl) or negative (Ttk and Yan) components of the RAS1 signaling pathway under GMR control, as well as other GMR constructs from different signaling pathways (Table 1). In addition, *lilli* mutants dominantly suppress the rough eye phenotypes of many *sE* transgenes (Dickson et al., 1992; Dickson et al.,

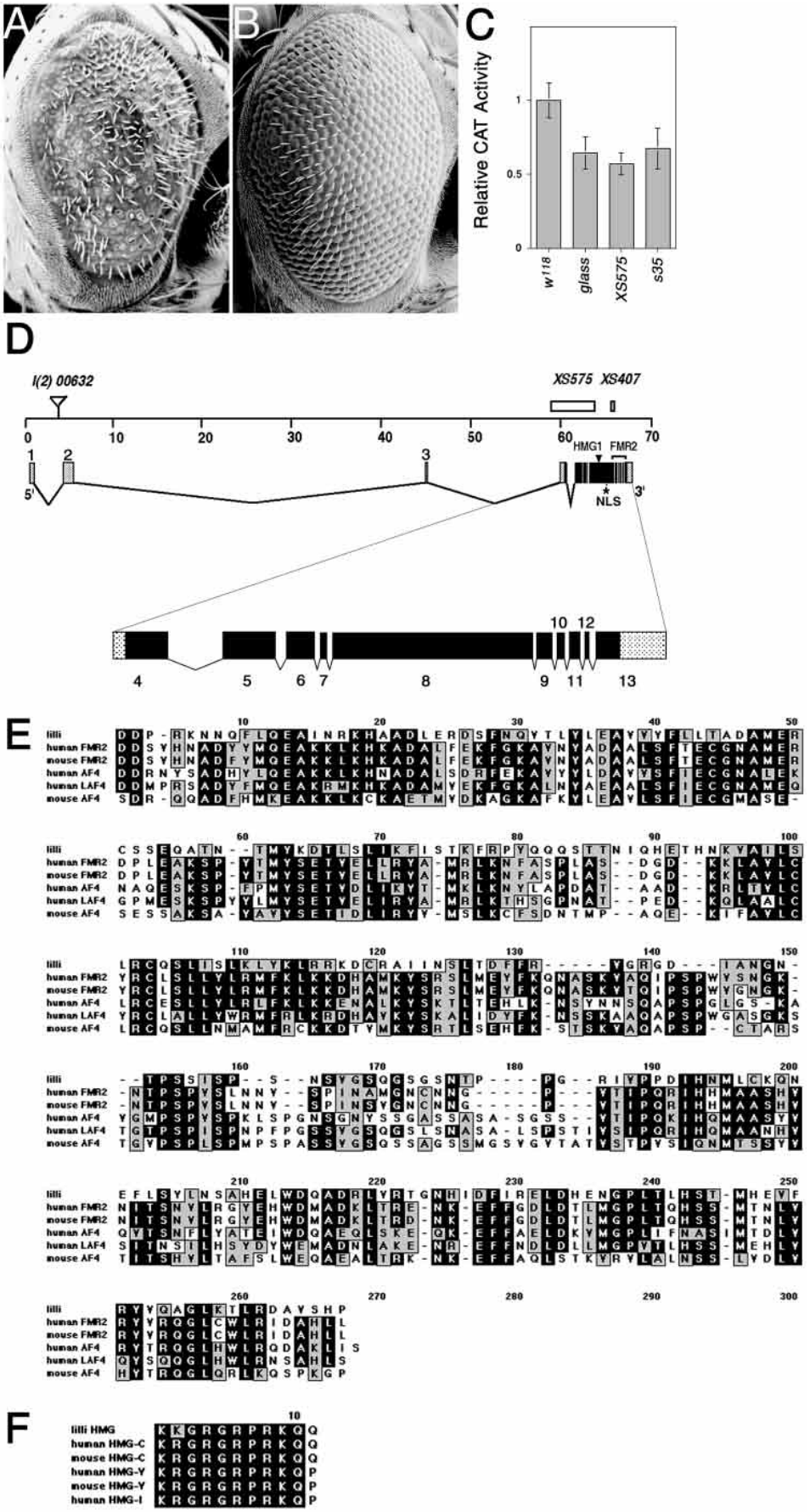

Fig. 1. *lilli* suppresses *GMR*-mediated expression and encodes a putative FMR2/AF4-like protein. Scanning electron micrographs (SEM) of adult eyes showing the screening for chromosome *GMR-phyl* alone (*CGP/+*) (A) and *GMR-phyl* in a *lilli* heterozygous background (*CGP/lilli*) (B). (C) The CAT activities from the *GMR-CAT* transgene were determined for third instar wandering larvae of specified genotypes of the heterozygotes: wild type (w^{118}), *glass*, $lilli^{XS575}$ *(XS575)* and $lilli^{s35}$ *(s35)*. The relative CAT activity was normalized to activity of the *GMR-CAT* transgene in wild type. A bar graph of the relative CAT activity is shown. Note that the suppression of CAT activity by *lilli* is comparable to that of *glass*. (D) Diagram of the *lilliputian* gene structure. The *lilli* cDNA and the direction of its transcription unit are indicated under the numbered line. The thirteen exons of the longest *lilli* transcript are depicted by boxes. The solid boxes represent *lilli*-coding regions and the dotted boxes represent untranslated regions. The FMR2 homology region is indicated by a bar that extends from the end of exon 8 into the end of exon 13. The HMG1 domain is indicated by a black arrowhead above exon 8. The nuclear localization signal (NLS) is indicated by an asterisk below exon 8. The P element $lilli^{l(2)00632}$ is inserted in the first intron of the gene (open inverted triangle). The DNA deleted from the *lilli*-coding region in two X-ray alleles, $lilli^{XS575}$ and $lilli^{XS407}$, are represented by open boxes above the numbered line. The allele $lilli^{XS575}$ is a 4,926 bp deletion that removes exon 4-8, including the translational start site. The allele $lilli^{XS407}$ is a 395 bp deletion that removes the 3′ end of exon 8 and introduces a premature stop codon 5 amino acids downstream of the 5′ breakpoint, thus truncating the open reading frame, including the entire FMR2 homology region. (E) Alignment of the FMR2 domains. The amino acid sequences from *Drosophila melanogaster*, human and mouse proteins were aligned using CLUSTAL-W. Lilli and the members of FMR2/AF4 proteins are homologous at their C-terminal regions. Amino acid residues shaded in black are identical and those shaded light gray are similar. (F) Alignment of the HMG-I/Y motif: Lilli has a highly conserved HMG motif.

Table 1. Summary of genetic interaction

Genotype	*lilli*^{XS575}	*lilli*^{XS407}	*lilli*^{s35}
GMR construct			
GMR-ras^{v12}*	S	S	S
GMR-phyl	S	S	S
GMR-sina	S	S	S
GMR-ttk^{88}	S	S	S
GMR-yan^{Act}	S	S	S
GMR-Rho^{1}*Rho*^{3}	S	S	S
GMR-reaper (III)	S	S	S
GMR-Dp110^{ACT}	S	S	S
GMR-Dp110$^{w.t.}$	S	S	S
GMR-Dp110^{DN}	S	S	S
sE construct			
sE-raf^{torY9}‡	S	S	S
sE-phyl	S	S	S
sE-ttk^{88}	S	S	S
sev construct			
sev-ras1^{v12}	E	E	E
sev-ras1^{N17} (III/III)§	0	0	0
sev-sem (III/III)¶	0	0	0
sev-phyl	0	0	0
sev-yan^{Act}	0	0	0
sev-notch^{Act}	0	0	0
sev-s11 (activated SEV)	0	0	0
mutant allele			
rl^{sem}	0	0	0
Ellipse (EGFR^{gof}*)*	E	E	E
raf^{HM7}**	–/0	–/0	–/0
Yan^{s2382}	0	0	0

Three different alleles of *lilli* were used in the genetic interaction tests. The suppression or enhancement in each genetic test was scored using the interaction with the w^{-}, isogenic 2:3 parental strain as a control. S, suppression; E, enhancement. 0, no effect, –/0, weak suppression or no effect.

sE (*sev* enhancer and *hs* basal promoter), *sev* (*sevenless* enhancer/promoter).

**Ras*^{V12}: a constitutively activated forms of *Ras1* (Fortini et al., 1992).

‡*Raf*^{torY9}: a constitutively activated form of Raf kinase (Dickson et al., 1992).

§*Ras*^{N17}: a dominant-negative form of *Ras1* (*Ras*^{N17}) (Feig and Cooper, 1988).

¶*rl*^{sem} (sem): A gain-of-function allele of *rolled/MAPK* (Brunner et al., 1994).

***raf*^{HM7}: a temperature-sensitive hypomorphic *raf* allele with reduced transcription from the *raf* gene (Dickson et al., 1992; Melnick et al., 1993).

1996), in which the *sevenless* enhancer is placed upstream of the *hsp70* basal promoter (Table 1).

These observations suggested that *lilli* was required, either directly or indirectly, for proper transcription from the *GMR* and *sE* expression constructs. Further supporting this hypothesis, we found that the levels of CAT activity from a *GMR-CAT* reporter construct (O'Neill and Rubin, unpublished reagents) were decreased by approx. 40% in third instar larvae heterozygous for *lilli* (Fig. 1C). Similar results were obtained when one copy of *glass*, a known activator of *GMR* transcription, was removed (O'Neill et al., 1995). These results suggest that *lilli* acts as a transcriptional regulator for *GMR* transgenes.

Molecular characterization of *lilli*

Previously, *lilli* was localized at 23C1-2 on the cytogenetic map, and the P element line *l(2)0632* was shown to fail to complement *lilli* mutant alleles (Neufeld et al., 1998b). We found that the lethality of *l(2)0632* could be reverted by P excision (77% (*n*=128) viable excisions recovered), indicating that the lethality corresponded to the P insertion site. Genomic fragments flanking the P element were isolated by plasmid rescue and used as probes to screen various cDNA libraries to isolate a large number of alternatively spliced cDNA clones, including one species that apparently encoded a full-length cDNA (Fig. 1D). Comparison of cDNA sequence to genomic sequence revealed a large transcription unit that spans approx. 68 kb (Fig. 1D). The gene contains 13 exons and the full-length *lilli* transcript is 8,516 bp in length. Conceptual translation of the open reading frame (ORF) yields a protein of 1,673 amino acids (Fig. 1D).

To determine whether this gene corresponded to *lilli*, genomic DNA was isolated from 4 EMS- and 19 X-ray-induced alleles, as well as 23 alleles induced by imprecise excision of *l(2)0632*. Southern blot analyses using the *lilli* ORF as a probe revealed polymorphisms in the coding region in several *lilli* mutant alleles, including two X-ray alleles, *XS575* and *XS407*, which contained deletions leading to truncated proteins (Fig. 1D). We rescued *lilli* mutants using the GAL4/UAS system (Brand and Perrimon, 1993) to express the full-length cDNA. Homozygous *lilli* mutants, which normally die as late embryos, survived to adulthood when they carried one copy each of *hs-GAL4* and *UAS-lilli* without heat shock treatment. No rescue was found in flies that carried *hs-GAL4* alone. Based on mutational analysis of the gene, viable excisions of the P line, and cDNA rescue, we conclude that this gene corresponds to *lilli*.

The predicted Lilli protein contains a high mobility group (HMG1) motif and a C-terminal domain present in the AF4 proto-oncoprotein and the human fragile X mental retardation protein FMR2 (Fig. 1E,F). Many HMG-containing proteins are DNA-binding, nonhistone nuclear proteins that interact with the minor groove of DNA (McGhee and Felsenfeld, 1980; Reeves and Nissen, 1990; Grosschedl et al., 1994). The FMR2/AF4-related gene family encodes nuclear proteins implicated in mental retardation (FMR2), cancer (AF4), and lymphocyte differentiation (LAF4) (Gu et al., 1992; Gu et al., 1996; Ma and Staudt, 1996; Gecz et al., 1996; Gecz et al., 1997; Chakrabarti and Davies, 1997; Taki et al., 1999). The presence of the HMG1 domain and FMR2 homology is consistent with the suggestion that Lilli acts as a transcription regulator.

lilli is a maternally provided pair-rule gene

To gain insight into its role during embryogenesis, we examined the phenotype of embryos mutant for *lilli*. Most embryos lacking zygotic *lilli* failed to hatch and subsequently died, although a small percentage hatched and died as first or second instar larvae. Cuticle from the late embryos was normal, with three thoracic and eight abdominal segments (Fig. 2A). Loss-of-function *lilli* mutations were found to be allelic to a lethal P-element insertion, *l(2)00632*, that exhibited a pair-rule-like segmentation phenotype when the maternal component of the gene was removed (Perrimon et al., 1996). Since both RNA in situ hybridization (data not shown) and the *l(2)00632* germline clone phenotype (Perrimon et al., 1996) suggested that *lilli* transcript is maternally contributed, we used the DFS-FLP technique to produce germline clones (GLC) that result in *lilli* null embryos that lack both maternal and zygotic Lilli activity (Chou and Perrimon, 1996).

lilli GLC embryos (*lilli*^{XS575} and *lilli*^{XS407}) exhibited pair-

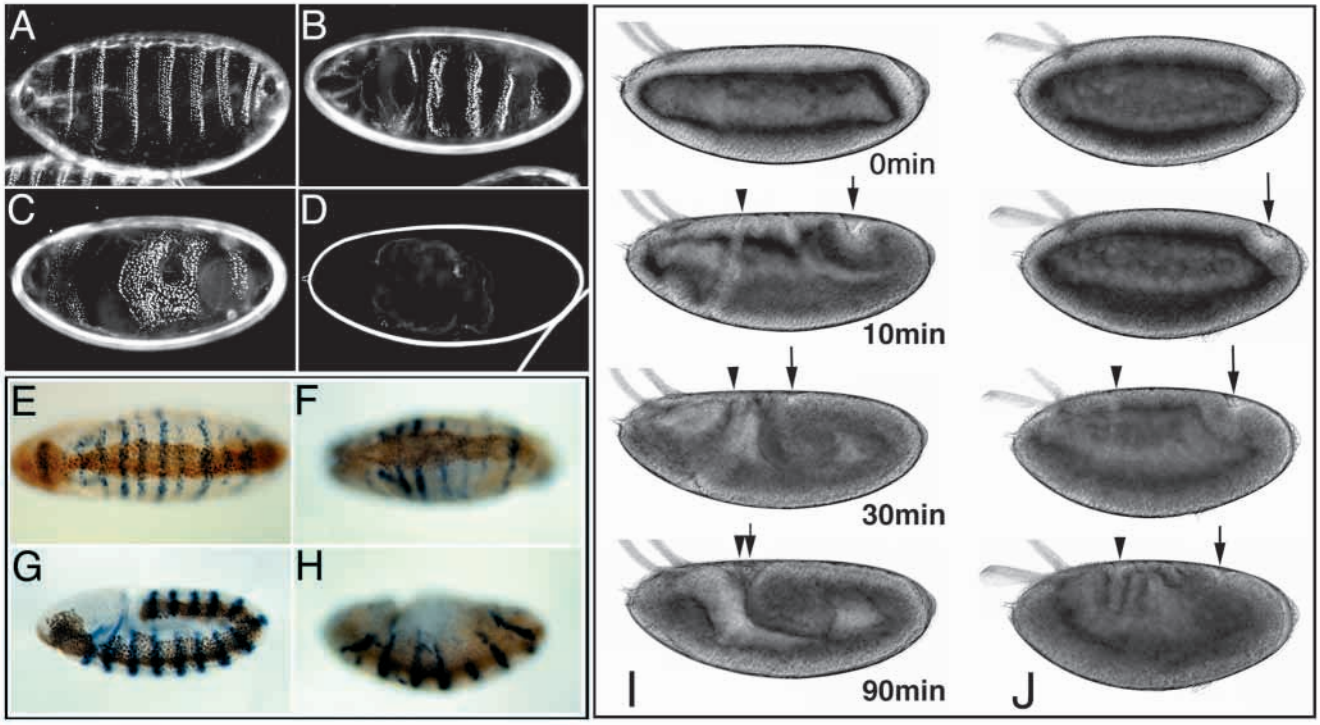

Fig. 2. Maternal expression of *lilli* is required for proper segmentation and germband extension. Dark-field micrographs of cuticle preparations from a zygotic *lilli*^{XS575} mutant embryo (A) and examples of the different phenotypes observed in *lilli*^{XS575} GLC embryos (B-D). A characteristic pair-rule defect is shown in B; a severe pair-rule defect with fused denticle belts in C; and an embryo with poor cuticle formation in D. (E-H) Immunolabeling of En (blue) and Twi (brown) proteins in wild type (E,G) and *lilli*^{XS575} GLC embryos (F,H). Embryos are shown in early germband extension stage 7/8 (E,F) and after germband extension (stage 9) (G,H). (I,J) The normal pattern of 14 En stripes is reduced to 7 stripes in *lilli* GLC embryos. Germband extension is compared between a wild-type (I) and a *lilli*^{XS575} GLC (J) embryo during gastrulation (the 0 min timemark is stage 6 (early gastrula) and the 90 min mark is stage 9 (extended germband stage). The position of the posterior end of the extending germband is marked with an arrow and the position of the cephalic furrow is marked with an arrowhead. In *lilli* GLC embryos, the initial extension of the germband is normal, but the second phase of germband extension is slow and eventually stops altogether. Note also in J that the formation of the cephalic furrow is also delayed in the *lilli* GLC embryos.

rule segmentation defects more severe than those previously reported for *lilli*$^{l(2)00632}$ (Fig. 2B-D; Perrimon et al., 1996). Two classes of phenotypes were observed. Approximately half of the embryos (52%; *n*=137) were missing odd numbered segments, with the remaining denticle belts often fused (44%; *n*=66) (Fig. 2B,C). The other class of *lilli* GLC embryos failed to secrete cuticle properly (Fig. 2D). These two phenotypic classes appear to reflect variation inherent to the *lilli* loss-of-function phenotype, rather than partial rescue by a paternal copy of *lilli*, as they were similarly observed whether wild-type or heterozygous *lilli* males were used. To further characterize these segmentation defects, we examined expression of the Engrailed (En) protein, which is present in 14 stripes along the anterior-posterior axis of wild-type embryos and marks the parasegment boundaries (DiNardo and O'Farrell, 1987; Fig. 2E,G). In *lilli* GLC embryos, the even-numbered En stripes were missing (Fig. 2F,H). Similar defects in Wingless expression were also observed (data not shown). Together, these results show that *lilli* is required for the establishment of odd-numbered segments in the embryo.

The activity of other known pair-rule genes is not only required for segmental patterning, but also for germband extension. Similarly, we found that germband extension is affected by loss of *lilli*. About 90 minutes after onset of gastrulation, germband extension in wild type reached 60% of dorsal egg length. In contrast, the germband never extended beyond 25% of dorsal egg length in *lilli* GLC embryos (Fig. 2I,J). These results suggest that *lilli* is required for the convergent extension movements during germband extension, consistent with its function as a maternally provided pair-rule gene.

ftz and *hkb* expression is altered in *lilli* GLC embryos

Given the potential role of *lilli* as a transcriptional regulator, we wished to examine whether the pair-rule phenotype in *lilli* GLC embryos corresponded to changes in the expression of early patterning genes. We therefore analyzed the spatiotemporal pattern of mRNA expression of several of these genes: the maternal coordinator gene *bicoid* (*bcd*); the gap gene *hunchback* (*hb*); the pair-rule genes *fushi tarazu* (*ftz*), *even-skipped* (*eve*), *hairy* (*h*), and *runt* (*run*); the segment polarity genes *engrailed* (*en*) and *wingless* (*wg*) and the terminal gap genes *tailless* (*tll*) and *huckebein* (*hkb*). The expression patterns of *bcd*, *hb*, *eve*, *h* and *run* mRNA appeared relatively normal (Fig. 3A,B,I-L; data not shown). In contrast, levels of *ftz* mRNA were significantly lower in *lilli* GLC embryos than wild-type embryos at the end of cellularization (Fig. 3E,F). *ftz* expression appeared normal prior to mid-cellularization (data not shown), after which its distribution became diffuse and

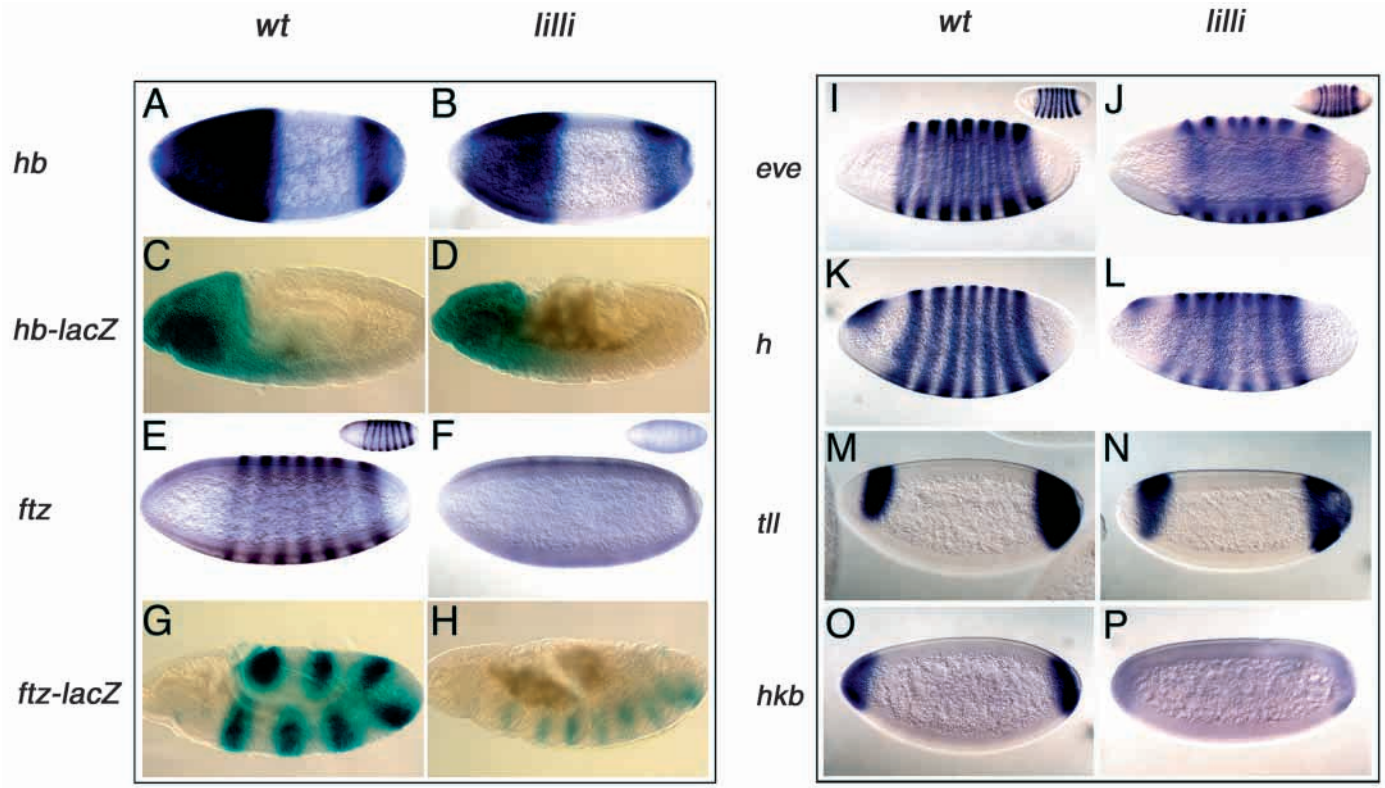

Fig. 3. Expression of the pair-rule gene *ftz* and of the terminal gap gene *hkb* are reduced in *lilli* GLC embryos. Expression of mRNA transcripts was detected by whole-mount in situ hybridization. The expression patterns of segmentation genes in wild-type (*wt*) embryos (A,E,I,K,M,O) are compared to those in *lilli* GLC embryos (*lilli*) (B, F, J, L, N, P) at cellularization blastoderm (stage 5) or early gastrula (stage 6). The probe used for RNA *in situ* hybridization is indicated in the left side of each individual panel. The small inserts in E and F represent surface views of the embryos. Note the major reductions in the expression levels of the *ftz* transcript (F) and the *hkb* transcript (P) in *lilli* GLC embryos. The expression patterns of the *hb-lacZ* transgene remained unaltered in wild-type embryos (C) and *lilli* GLC embryos (D), while that of the *ftz-lacZ* transgene is markedly reduced in *lilli* GLC embryos (G,H). All embryos are oriented with anterior to the left and dorsal side up.

uniform, and it rarely accumulated in stripes (Fig. 3F). Using *ftz-lacZ* and *hb-lacZ* transgenes to determine the level of such regulation, we found that expression of the *ftz-lacZ* transgene was markedly reduced in *lilli* GLC embryos, while that of the *hb-lacZ* transgene remained unimpaired (Fig. 3C,D,G,H). This suggests that Lilli regulates *ftz* gene expression at the transcriptional level. Since both *ftz* and *lilli* are required for even-numbered En stripes and odd-numbered segment formation (DiNardo and O'Farrell, 1987), this disruption of *ftz* expression may account for the pair-rule phenotype observed in *lilli* GLC embryos.

In addition, we found that *hkb* mRNA was either reduced or absent at the embryonic termini, while the expression of *tll* mRNA was largely unaffected in *lilli* GLC embryos (Fig. 3M-P). *hkb* establishes the anterior and posterior borders of the ventral furrow during gastrulation (Reuter and Leptin, 1994), and lack of *hkb* expression causes the mesoderm and ventral domain to extend to the poles; this domain is marked by expression of *snail* (*sna*). Accordingly, we found a small extension of the ventral domain that expresses *sna* and undergoes ventral furrow formation (data not shown).

lilli is required for cytoskeletal functions during cellularization

The significant percentage of embryos that failed to properly secrete cuticle (see above) suggested that *lilli* GLC embryos had defects in addition to the patterning defects described above. We first examined cytoskeletal architecture integrity during cellularization. In wild-type embryos, early in cellularization the distribution of actin filaments changes from an apical cortical cap to an apical internuclear position (Schejter and Wieschaus, 1993a; Fig. 4A,B). Following this initial phase of cellularization, nuclei elongate and microtubules form characteristic arrays described as perinuclear inverted baskets, while actin filaments maintain a contractile regular network of hexagonal units surrounding the microtubular arrays (Fig. 4C-E). Toward the end of cellularization, the individual units of the actin network contract and the resulting cells retain thin connections, called yolk stalks, to the center of the embryo (Schejter and Wieschaus, 1993a; Fig. 4K,L).

lilli GLC embryos exhibited specific defects in the maintenance of the actin network during cellularization. The initial phase of cellularization occurred normally (Fig. 4F,G). However, during the second phase of cellularization, specific defects in the maintenance of the contractile actin network were observed, as the actin network began to contract and the furrow tips moved basally. The actin filaments became unevenly distributed between nuclei, ranging from abnormally large bundles to regions where the actin network was thin or

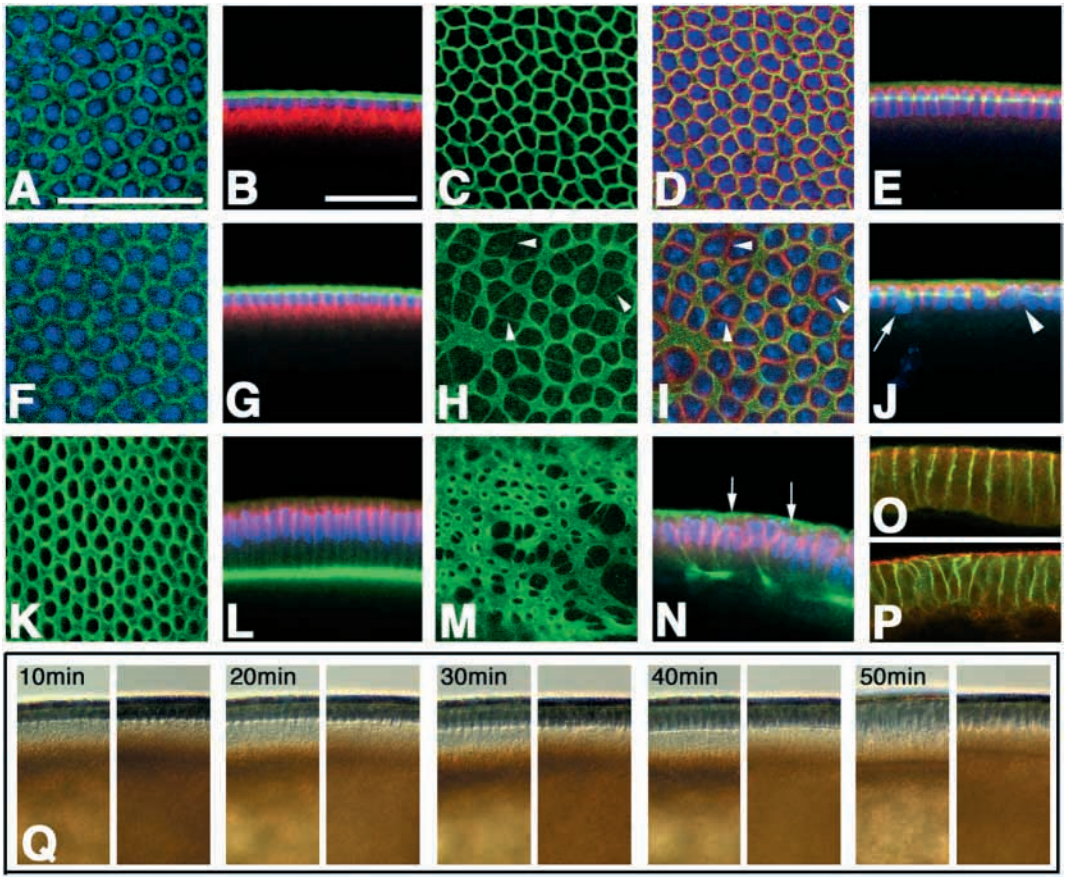

Fig. 4. Lilli is required for the maintenance of the hexagonal actin network and for lipid droplet clearing from the cortex during cellularization. Confocal images of embryos during cellularization stained with Phalloidin for F-actin (green), α-tubulin antibody for microtubules (red) and YOYO-1™ for DNA (blue). (A-N) F-actin, α-tubulin, DNA triple labeling; (O-P) Armadillo, neurotactin double labeling. (A,B) A wild-type embryo early during slow phase of cellularization at the time when actin redistributes from apical caps to internuclear regions. (A) A surface view focusing on the apical internuclear space. (B) A cross section of the same embryo. (F,G) Images of a *lilli*^{XS575} GLC embryo taken at a similar stage. (C-E) Wild-type embryos during the slow phase of cellularization. (H-J) *lilli*^{XS575} GLC embryos at the same stage as in C-E. The actin bundles are uneven in thickness and are frequently absent between two or more nuclei (arrowheads in H), although the distribution of the microtubules is mostly normal (arrowhead in I). (J) The absence of F-actin accumulation at the furrow tips is seen in cross section (arrowhead). Occasionally, nuclei are found in more basal cortical regions (arrow). (K,L) Wild-type embryo at the end of cellularization. K focuses on the base of the furrows. In cross section (L) F-actin is seen concentrated at the base of the blastoderm epithelium. (M) In *lilli*^{XS575} GLC embryos, yolk stalks exhibit highly irregular outlines. (N) In cross section, multinucleated cells can be seen (arrow), although each nucleus in these cells remain surrounded by a characteristic inverted basket array of microtubules. Note that F-actin is also concentrated in the apical cortex of the cells. (O,P) Confocal images of early gastrula stage embryos (stage 7) stained with antibodies against Armadillo protein (red) and neurotactin (green). Cross sections through the dorsolateral ectoderm are shown. Arm is localized to adherens junctions and neurotactin is a marker for the basolateral membrane domains in both wild-type and *lilli* GLC embryos. Scale bars in A and B are 20 μm and apply for all images (surface views and cross sections, respectively). (Q) High magnification views of the cortical cytoplasm of living wild-type (left hand panels) and *lilli* GLC (right hand panels) embryos. Embryos were staged by observation under halocarbon oil, mounted for video microscopy and imaged at 10 minute intervals. After 40 minutes into cycle 14, lipid droplets are normally cleared by microtubule-dependent bulk movement from the cortex establishing a region of clear cytoplasm basal to the nuclei (gray in color). In *lilli* GLC embryos lipid droplets remain distributed throughout the cortical cytoplasm even 40 minutes after the onset of cycle 14.

absent (Fig. 4H-J), resulting in multinucleated cells (Fig. 4H,J). The microtubular baskets surrounding each nucleus appeared largely normal, even in regions where actin filaments were unevenly distributed (Fig. 4I). At the end of cellularization, the yolk stalks were irregular in shape and size, and large connections between cortical cells and the central yolk cell were frequently seen (Fig. 4M,N). Despite these defects, video-timelapse analysis revealed that the timing of cellularization and membrane formation was unimpaired in *lilli* GLC embryos (data not shown) and did result in an epithelial monolayer of cells with proper apical-basal polarity (Fig. 4O,P).

In addition to the failure in maintaining the actin network, *lilli* GLC embryos exhibited defects in transport of organelles during cellularization (Fig. 4Q). In wild-type embryos, lipid droplets move along microtubules in a bi-directional fashion and accumulate basally during cycle 14, near the plus ends of microtubules (Welte et al., 1998; Gross et al., 2000). As the cortical cytoplasm becomes depleted of lipid droplets, it appears transparent (Welte et al., 1998; Fig. 4Q). In *lilli* GLC embryos, this cortical clearing is perturbed, resulting in a 'halo' of non-cleared cytoplasm around the central yolk (Fig. 4Q). Living *lilli* GLC embryos were found to have abnormal distribution of lipid droplets during cellularization (Fig. 4Q) and about 80% (n=56) of the embryos failed to separate from the central yolk sac shortly after cellularization. To determine whether this failure to clear was caused by a general breakdown of cytoplasmic transport, we examined the transport of yolk vesicles and the integrity of the microtubule network. The distribution of yolk vesicles can be observed in fixed embryos following extraction of neutral lipid from the lipid droplets. In *lilli* GLC embryos, yolk vesicle movement was normal during cellularization (Fig. 5B), and the general distribution of microtubular arrays was largely unaffected (Fig.

4I). Thus, *lilli* does not induce general breakdown of microtubule-based transport, but rather is required specifically for the microtubule-based basal transport of lipid droplets.

lilli is required for the expression of *Sry* α, a zygotic regulator of the actin cytoskeleton

Pan-genomic zygotic screens for genes that are required for proper function of the actin network during cellularization have identified three genes, *nullo*, *Sry α* and *bnk* (Merrill et al., 1988; Wieschaus and Sweeton, 1988). The cellularization phenotypes of *lilli* GLC embryos are similar to those observed for mutations in the blastoderm-specific genes *nullo* and *Sry α* (Schweisguth et al., 1990; Simpson and Wieschaus, 1990; Simpson-Rose and Wieschaus, 1992). In contrast, mutations in *bnk* disrupt the timing of microfilament rearrangement during cellularization (Schejter and Wieschaus, 1993b). We used antibodies against the Nullo and Bnk proteins to examine their distribution in *lilli* GLC embryos. In wild-type embryos, Nullo and Bnk proteins colocalize with filamentous actin at the leading edge of the invaginating furrows at mid-cellularization (Fig. 5E,F,I,J). In *lilli* GLC embryos, Nullo and Bnk were expressed and localized normally, although the vesicular Nullo staining in the basal periplasm was somewhat less pronounced (Fig. 5G,H,K,L). In grazing sections, the alterations observed in Nullo and Bnk distribution likely reflected the disruptions of the actin network (Fig. 5G,K). Thus, we conclude that the cellularization defects in *lilli* GLC embryos cannot be attributed to lack of Nullo or Bnk expression.

Sry α mRNA is normally expressed at low and uniform levels at cycle 13, and is then concentrated in two broad bands prior to its down regulation late in cycle 14 (Fig. 5A; Ibnsouda et al., 1993). Interestingly, we were unable to detect expression of the *Sry α* gene during cellularization in *lilli* GLC embryos (Fig. 5B). Expression of a *Sry-lacZ* transgene was likewise abolished in *lilli* GLC embryos (Fig. 5D), indicating that the defect in *Sry α* expression is at the transcriptional level. Since the mutant phenotype of *Sry α* is very similar to that of *lilli* GLC embryos, it seems likely that the cellularization defects observed in *lilli* GLC embryos are caused, at least in part, by a strong reduction in *Sry α* expression.

Mutations in *lilli* reduce cell size but not growth rate

In previous studies, we found that retinal cells lacking *lilli* were significantly smaller than wild-type cells (Neufeld et al., 1998b). Recently, mutations in a number of components of a PI3K-dependent signaling pathway have been shown to reduce the size of a variety of cell types in *Drosophila* (Böhni et al., 1999; Chen et al., 1996; Montagne et al., 1999; Verdu et al., 1999; Weinkove et al., 1999; Zhang et al., 2000). The reduced cell size of these mutants reflects an underlying reduction in the rate of cellular growth, and thus inhibition of this pathway can lead to reductions in the size of mutant clones, organs, or animals (Conlon and Raff, 1999; Lehner, 1999; Edgar, 1999; Weinkove and Leevers, 2000). In contrast, despite the small size of individual *lilli* mutant adult cells, we found that we could generate relatively large clones of *lilli* mutant cells (Figs 6A and 7A), suggesting that *lilli* may affect cell size without changing the overall rate of growth. This was tested by comparing the size of individual *lilli* mutant clones to their wild-type twinspots in third instar eye and wing imaginal discs. We found that *lilli* clones induced either at 24-36 hours or 36-48 hours after egg deposition (AED) were indistinguishable in size and number of cells from their wild-type twinspots. Of 75 individual clones examined at 96 hours after induction, the average area of *lilli* mutant clones was 1440 pixels, compared to 1400 pixels for corresponding wild-type twinspots (Fig. 6B). Thus, *lilli* mutant cells grew at 1.03 (±0.57) times the rate of wild-type cells, indicating that *lilli* is not required for normal rates of cell growth.

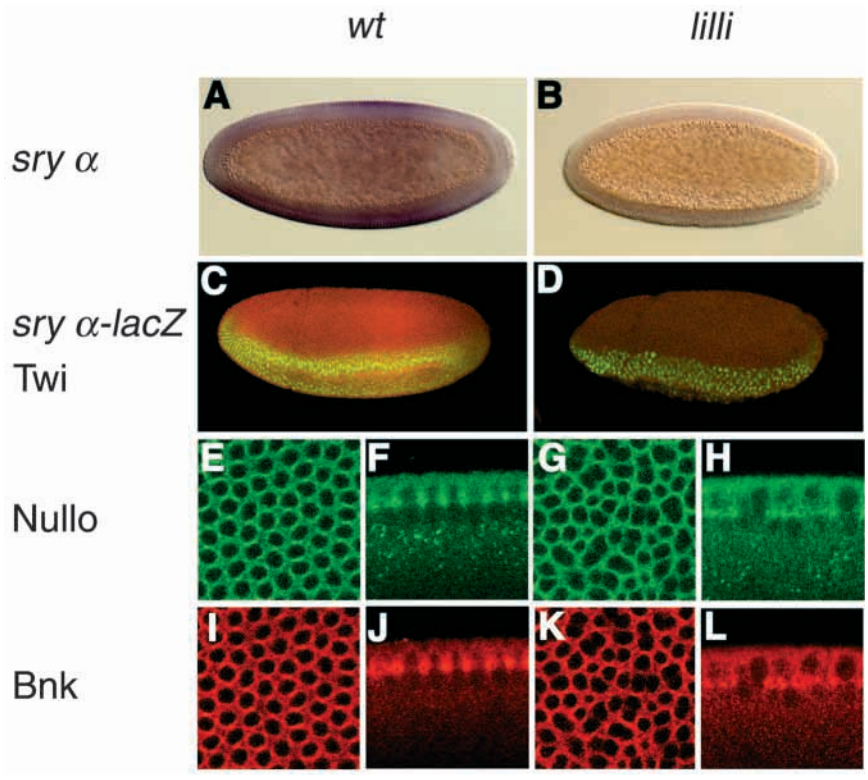

Fig. 5. Expression of zygotic regulators of cellularization in *lilli* GLC embryos. (A,B) Expression of *Sry α* transcripts detected by in situ hybridization during mid cellularization. In wild-type (A), *Sry α* transcripts are localized in a broad band in the trunk and a smaller band in the anterior region. Note the absence of endogenous *Sry α* transcripts in *lilli* GLC embryos derived from two different mutant alleles, *lilli*^{XS575} (B) and *lilli*^{XS407} (data not shown). (C,D) Expression of β-galactosidase expression (red) in wild-type (C) and *lilli* GLC (D) embryos carrying a *Sry α-lacZ* transgene. Expression of Twist protein (green) is shown as a control. Note the absence of *Sry α-lacZ* expression in *lilli* GLC embryos. (E-H) The immunolabeling of Nullo protein (green) and (I-L) Bnk protein localization (red) in blastoderm embryos at mid cellularization. (E,F,I,J) Wild-type embryos; (G,H,K,L) *lilli*^{XS575} GLC embryos. (E,I,G,K) Grazing sections, (F,J,H,L) cross sections through the advancing furrow membranes. Note, in *lilli* GLC embryos, disruptions of the regular pattern of the leading edges of the furrow membranes. The distribution of yolk platelets in *lilli* GLC embryos is unimpaired.

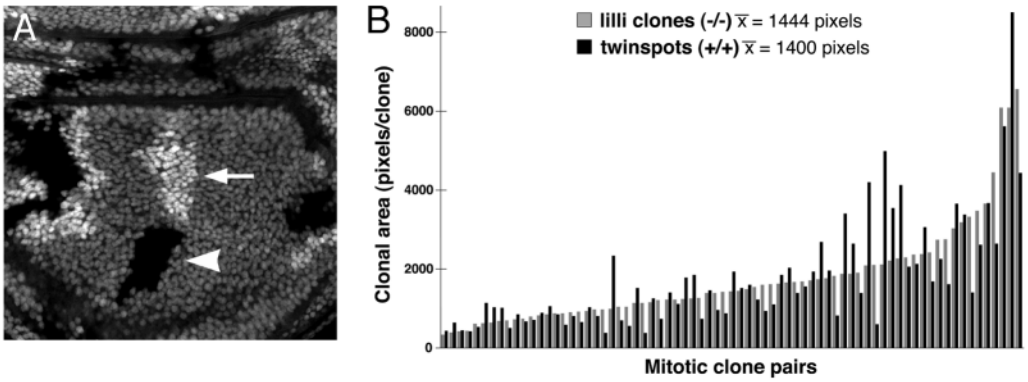

Fig. 6. Loss of *lilli* does not affect cellular growth rate. (A) Confocal image of a third instar imaginal wing disc containing pairs of *lilli*^{XS575} mutant clones (arrowhead; mutant cells lack GFP marker) and their corresponding wild-type twinspots (arrow; cells contain two copies of GFP marker). Clones were induced at 24-36 hours AED, and discs were fixed 96 hours after clone induction. Note the similar size of mutant and twinspot clones. Genotype: *y, w, HS-flp; lilli*^{XS575} *FRT40A/UbiGFP FRT40A*. (B) Graph showing relative sizes (clone areas) of 75 individual pairs of *lilli*^{XS575} mutant clones (gray bars) and wild-type twinspots (black bars), induced as in A. The average ratio of the areas of *lilli* clones to wild-type clones is 1.03±0.57, indicating a normal rate of growth in *lilli* mutant cells.

Interestingly, despite an approximately 50% reduction in the size of *lilli* photoreceptor cells and wing margin bristles in the adult (Fig. 7A,B), other cell types in the adult eye and wing were unaffected. For example, the surface of eyes containing *lilli* mutant clones appeared normal by SEM analysis (data not shown), suggesting that loss of *lilli* did not reduce the size of cone cells. The size of *lilli* cells in developing wing and eye imaginal discs appeared normal as well (Fig. 7C and data not shown). This was confirmed by FACS analysis of dissociated wing discs, which revealed no significant difference in size between *lilli* and wild-type cells (Fig. 7D). In addition, unlike mutations in components of the PI3K pathway, *lilli* mutant cells displayed a normal cell cycle profile (Fig. 7E). To test whether *lilli* is required for PI3K-mediated growth, we examined cells doubly mutant for *lilli* and *Pten*, an inhibitor of this pathway. Mutations in *Pten* increase cell size and advance G_1/S progression (Goberdhan et al., 1999; Huang et al., 1999; Gao et al., 2000); these effects are prevented by mutations in

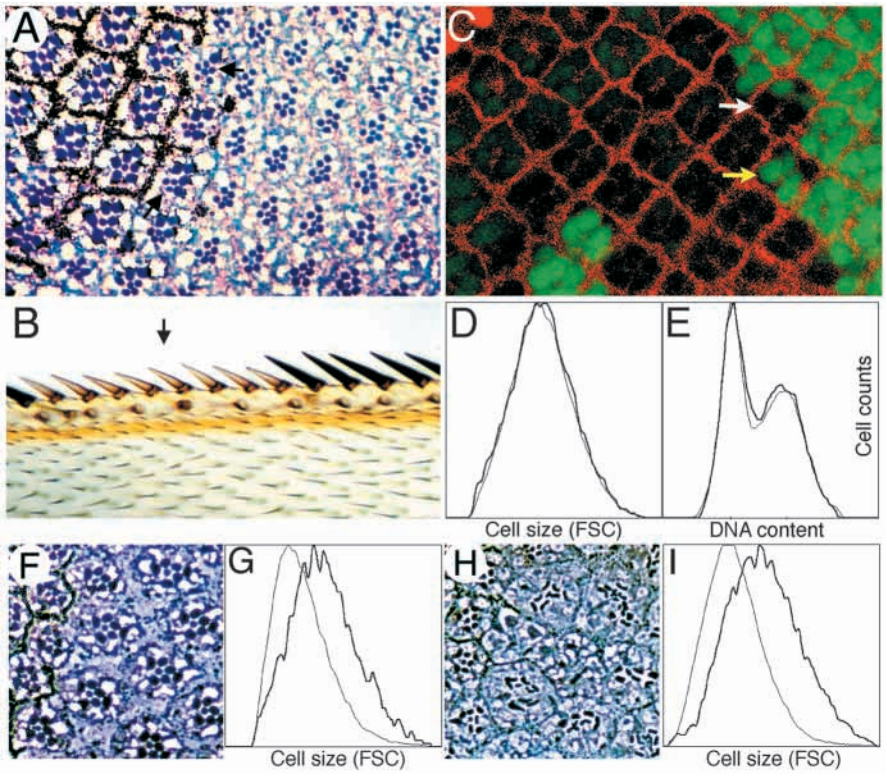

Fig. 7. Mutations in *lilli* decrease the size of specific adult cell types. (A) Tangential section through a *lilli*^{XS575} homozygous clone in an adult retina. The mutant clone is marked by the absence of pigment (w^+). Mutant photoreceptor cells are smaller when compared to heterozygous photoreceptor cells. At the clone border, mosaic ommatidia containing a mixture of pigmented wild-type and unpigmented *lilli* mutant cells are evident. Note that only the *lilli* photoreceptor cells in mosaic ommatidia (black arrows) are reduced in size, indicating cell autonomy. Homozygous mutant clones of the *lilli*^{XS407} allele gave identical clonal phenotypes (data not shown). (B) Adult wing margin carrying a *lilli*^{XS575} homozygous mutant clone. Note that *lilli* homozygous mutant bristles marked by *yellow* (indicated by a black arrow) are shorter than wild-type bristles, which have a dark color. (C) Confocal micrograph of a third instar larval eye imaginal disc containing *lilli* mutant clones. Homozygous mutant clones are marked by the absence of GFP staining (green). The twinspots are marked by the brighter GFP staining in the adjacent area. The disc was also stained with the F-actin binding molecule TRITC-Phalloidin (red). Note that there are no observed differences in cell size and between the *lilli*^{XS575} clones and their corresponding twinspots (white arrow and yellow arrow). (D,E) FACS analysis of dissociated third instar wing discs containing clones of *lilli*^{XS575}. Dark traces represent mutant cells, while light traces represent control cells from the same discs. (D) Forward light scatter value (FSC) is a measure of cell size. No significant difference in size is detected between wild-type and *lilli* mutant cells. (E) Comparison of DNA content indicates cell cycle phasing is also unaffected by loss of *lilli*. (F-I) Genetic interactions between *lilli* and *Pten*. Adult eye sections (F,H) and FACS analysis (G,I) of wing disc cells. Dark traces represent mutant cells; light traces represent controls. As described previously, mutations in *Pten* lead to cell enlargement (F,G). Cells doubly mutant for *lilli* and *Pten* (H,I) enlarge to the same extent as *dPTEN* single mutant cells; ommatidia of this genotype appear disorganized.

downstream components such as *torso* (*tor*/*dTOR*; Zhang et al., 2000). In contrast, loss of *lilli* did not prevent the cell enlargement or cell cycle changes caused by *Pten* mutation (Fig. 7F-7I and data not shown), indicating that *lilli* is not an essential element of the PI3K pathway. Interestingly, we noticed that ommatidia containing the enlarged *lilli Pten* photoreceptor cells were severely disorganized, and contained malformed rhabdomeres characteristic of cytoskeletal defects (Fig. 7H; Fischer-Vize and Mosley, 1994; Fan and Ready, 1997). Together, these results indicate that *lilli* affects the cell size through a growth-independent and PI3K-independent mechanism. We suggest that mutations in *lilli* may affect final cell size by disrupting the morphological changes that cells such as rhabdomeres and bristles, which are the specializations of photoreceptor and trochogen cells respectively, undergo during pupal development.

DISCUSSION

lilli is a maternally provided pair-rule gene

Four lines of evidence support the idea that *lilli* functions during embryogenesis as a maternally contributed pair-rule gene: *lilli* GLC embryos fail to establish even-number En stripes; they subsequently lack odd-number segments; they exhibit defects in germband extension, and these phenotypes are not seen in homozygous *lilli* embryos lacking zygotic Lilli function. Thus, our results demonstrate that Lilli is required maternally for normal segmentation during embryogenesis.

What is the mode of action of *lilli* in segmentation? Unlike zygotic pair-rule genes that are expressed in the trunk region of the embryo in seven stripes (St Johnson and Nüsslein-Volhard, 1992; Ingham and Martinez Arias, 1992), the expression pattern of *lilli* transcript is not segmental. Thus, *lilli* may play a role in the expression, localization or activity of other pair-rule genes. *lilli* probably does not act through the major gap genes *knirps* (*kni*), *Krüppel* (*Kr*), or *giant* (*gt*), because the striped pattern of the primary pair-rule genes *eve*, *h* and *run* are unaffected in *lilli* GLC embryos (Nüsslein-Volhard and Wieschaus, 1980; St. Johnson and Nüsslein-Volhard, 1992; Ingham and Martinez Arias, 1992).

One function of *lilli* is to regulate *ftz* transcription, since expression of both endogenous *ftz* mRNA and a *ftz-lacZ* transgene are markedly reduced in *lilli* GLC embryos. Although a low level of *ftz* mRNA remains in *lilli* GLC embryos, these transcripts never resolve into seven stripes. It is possible that *lilli* directly regulates *ftz* transcription in combination with other transcription and regulatory factors, or that *lilli* is required for the function or expression of such molecules. A candidate for such a factor is the product of the *ftz-f1* gene, which was shown to be required maternally for *ftz* expression (Guichet et al., 1997; Yu et al., 1997).

While the developmental defects observed in *lilli* GLC embryos are largely consistent with *ftz* being the primary target of *lilli*, *ftz* mutant embryos do not exhibit defects in germband extension movements as strong as those observed in *lilli* GLC embryos (Irvine and Wieschaus, 1994). The only other known gene that is necessary for germband extension is that of the *Drosophila* $5HT_2$-serotonin receptor ($5HT_2$-SR) (Colas et al., 1999). The function of $5HT_2$-SR during germband extension is unclear, but since its segmental expression is indispensable for cell intercalation movements in the germband it may provide another possible target for *lilli* function. Further analysis of *lilli* targets is likely to result in the identification of genes that govern germband extension movements during gastrulation.

lilli is essential for cytoskeletal functions during cellularization

Genetic studies have indicated that cellularization specifically requires a relatively small number of zygotically active genes, including *Sry* α, *nullo* and *bnk* (Merrill et al., 1988; Wieschaus and Sweeton, 1988). Removal of the maternal contribution of *lilli* phenocopies the cellularization defects observed in zygotic mutation in either *Sry* α or *nullo* (Simpson and Wieschaus, 1990, Schweisguth et al., 1990). *lilli* thus represents the first identified gene that is required maternally for specific cytoskeletal functions at the onset of zygotic gene activity at mitotic cycle 14. Our results suggest that *Sry* α is another primary target of *lilli* function. First, in both *lilli* and *Sry* α mutant embryos Nullo protein distribution is normal, except where the actin network is disrupted (Postner and Wieschaus, 1994). Second, *lilli* regulates *Sry* expression at the transcription level, since both *Sry* mRNA expression and *Sry-lacZ* transgene expression are absent in the blastoderm in *lilli* GLC embryos, suggesting that this may be the primary cause for the cellularization defects observed in *lilli* GLC embryos.

Vesicle transport is a tightly regulated process during early development and depends on maternal and zygotic gene function (Welte et al., 1998). The basal movement of the lipid droplets during mitotic cycle 14 is mediated by a microtubule-dependent transport mechanism (Welte et al., 1998; Gross et al., 2000). Because lipid droplet transport is disrupted in *lilli* GLC embryos, *lilli* is also required for at least one microtubule-dependent transport process. Mutations in only one other locus, *halo*, cause a specific defect in cortical clearing similar to that of *lilli*. Since microtubule function and structure appears otherwise normal in *lilli* GLC embryos, *lilli* may be required for the expression and function of Halo, or other unidentified components of lipid droplet transport machinery. The molecular nature of Halo is not known and mutations are not available to examine potential genetic interaction with *lilli*.

lilli and regulation of cell size

One of the most striking aspects of the *lilli* mutant phenotype is the marked reduction in size of *lilli* mutant cells. Recently, a number of components of the PI3K-mediated signaling pathway have been shown to regulate cell size in *Drosophila*. Loss-of-function mutations in *Insulin-like receptor* (Chen et al., 1996), the insulin receptor substrate homolog *chico* (Böhni et al., 1999), PI3K subunits *Dp110* and *Dp60* (Weinkove et al., 1999), *Dakt1* (*Akt1*; Verdu et al., 1999), *tor*/*dTOR* (Zhang et al., 2000), and *dS6K* (*S6k*; Montagne et al., 1999) each cause cell size changes similar to those which we observe in *lilli* mutant cells. This apparent phenotypic similarity is consistent with *lilli* regulating cell growth by modulating PI3K signaling, or by acting as a target of the PI3K pathway. However, *lilli* differs from these and other growth regulators in a number of significant ways. First, the reduction in cell size caused by loss of PI3K signaling is associated with an overall reduction in growth and proliferation, such that clones of mutant cells grow

more slowly than their wild-type twinspots. In contrast, we found that *lilli* mutant cells proliferated to the same extent as wild-type cells, and could give rise to large clones encompassing a significant fraction of the adult eye. Second, whereas mutations in components of the PI3K signaling pathway reduce the size of both adult and imaginal disc cells, loss of *lilli* did not affect cell size in imaginal discs. Third, overexpression of *Dp110, Dakt1* or *dS6K* leads to marked increases in cell and organ size, whereas overexpression of *lilli* actually decreased the size of retinal cells and bristles (data not shown). Together, these results argue that the reduced size of *lilli* mutant cells is not the result of defective growth, and that *lilli* does not function to regulate cell growth.

How then might *lilli* affect cell size? One plausible theory is suggested by the observation that *lilli* mutations have a disproportionate effect on cells with specialized structures such as rhabdomeres and bristles, while epithelial cells are largely unaffected. Rather than regulating cell growth, *lilli* may be required to organize such cellular structures. Given the extensive cytoskeletal rearrangements necessary to elaborate a rhabdomere or bristle, such a role would fit with the observed cytoskeletal defects in *lilli* GLC embryos. The phenotype of cells doubly mutant for *lilli* and *dPTEN* also supports this view: *lilli* was not required for the cellular hypertrophy caused by mutations in *dPTEN*, but the cytoarchitecture of the enlarged double mutant cells was disrupted. Thus, some of *lilli*'s functions may only be evident in cells in which great demands are placed on the cytoskeleton. Alternatively, *lilli* may be part of a mechanism that governs postmitotic cell size independently of growth signals.

lilli and transcriptional regulation

Our genetic studies demonstrate that mutations in *lilli* disrupt the expression pattern of a subset of early patterning zygotic genes, including *ftz, hkb,* and *Sry α.* In addition, *lilli* mutants dominantly suppress expression from *GMR* and *sE* transgenes, both of which share a common promoter element. As most genes examined had largely normal expression in *lilli* GLC embryos, it is unlikely that Lilli is generally required for efficient transcription. A more likely explanation is that *lilli* specifically regulates the transcription of a limited subset of genes including *ftz*, *hkb*, and *Sry α.*

While both *hkb* and *tll* encode transcription factors that regulate terminal structure differentiation and are induced by the receptor tyrosine kinase Torso (Tor; reviewed in Lu et al., 1993; Duffy and Perrimon, 1994), *hkb* but not *tll* expression is strongly reduced in *lilli* GLC embryos. One difference between the two transcription factors is that low levels of Tor signaling induce *tll* expression, whereas higher levels are required for expression of *hkb* (Greenwood and Struhl, 1997). Thus one possibility is that *lilli* is required for translating the quantitative differences of Torso/Ras signaling into distinct expression patterns of these two transcription factors.

Based on our data, we propose that Lilli acts as a cofactor for zygotically expressed transcription factor(s). In such a model, Lilli would provide specificity to a more general zygotic factor, while this factor itself would provide the correct timing of transcriptional regulation. It is striking that genes like *bnk*, *Sry α*, and *nullo*, which have remarkably similar expression patterns and embryonic functions, exhibit different requirements for *lilli* action. While we have identified three potential targets of *lilli* function, there are defects in *lilli* GLC embryos that cannot be explained by misregulation of any known genes. The identification of new *lilli* targets will help to identify key regulatory genes involved in processes such as lipid droplet transport and germband extension movements, and may also provide functional cues to the family of the FMR2/AF4-like proteins.

Correspondence should be addressed to A.H.T. and H.A.M. We thank E. Hafen, F. Wittwer, and S. Newfeld for communication prior to publication. We thank C. Goodman, M. Frasch, S. Roth, E. Scheijter, and E. Wieschaus for antibodies. We thank Z. Zhou, H. Zhang, M. Brodsky, E. Schejter, A. Stathopoulos and A. Vincent for cDNA and RNA probes. The authors thank S. Mullaney for assistance with P-element mediated transformation, M. Evans-Holm and G. Tsang for assistance with DNA sequencing, S. Ruzin and A. Grimm for expert technical assistance with Zeiss Confocal microscopy. We are grateful to E. Wieschaus, M. Levine, K. M. C. Sullivan, T. Serano, B. A. Hay, M. Welte, T. Blankenship, E. Frise, A. Stathopoulos and A. Bailey for critical reading of this manuscript, and our colleagues, K. M. C. Sullivan, T. Serano, B. A. Hay, M. Therrien, F. D. Karim and D. Wasserman for helpful discussions. H. A. M. thanks E. Knust, E. Schejter, A. Vincent, M. Welte and A. Wodarz for discussions. A. H. T. is supported by a senior postdoctoral fellowship from the Leukemia and Lymphoma Society. H. A. M. is supported by the Deutsche Forschungsgemeinschaft.

REFERENCES

Böhni R., Riesgo-Escovar, J., Oldham, S., Brogiolo, W., Stocker, H., Andruss, B. F., Beckingham, K. and Hafen, E. (1999). Autonomous control of cell and organ size by CHICO, a *Drosophila* homolog of vertebrate IRS1-4. *Cell* **97**, 865-875.

Brand, A. and Perrimon, N. (1993). Targeted gene expression as a means of altering cell fates and generating dominant phenotypes. *Development* **118**, 401–415.

Brunner, D., Ducker, K., Oellers, N., Hafen, E., Scholz, H. and Klambt, C. (1994). The ETS domain protein Pointed-P2 is a target of MAP kinase in the Sevenless signal transduction pathway. *Nature* **370**, 386-389.

Chakrabarti, L. and Davies, K. E. (1997). Fragile X syndrome. *Curr. Opin. Neurol.* **10**, 142-147.

Chang, H. C., Solomon, N. M., Wassarman, D. A., Karim, F. D., Therrien, M., Rubin, G. M. and Wolff, T. (1995). *phyllopod* functions in the fate determination of a subset of photoreceptors in *Drosophila Cell* **80**, 463.

Chen, C., Jack, J. and Garofalo, R. S. (1996). The *Drosophila* insulin receptor is required for normal growth. *Endocrinology* **137**, 846-856.

Chou, T. B. and Perrimon, N. (1996). The autosomal FLP-DFS technique for generating germline mosaics in *Drosophila melanogaster*. *Genetics* **144**, 1673-1679.

Colas, J. F., Launay, J.-M., Vonesch, J.-L., Hickel, P. and Maroteaux, L. (1999). Serotonin synchronizes convergent extension of ectoderm with morphogenetic gastrulation movements in *Drosophila*. *Mech. Dev.* **87**, 77-91.

Conlon, I. and Raff, M. (1999). Size control in animal development. *Cell* **96**, 235-244.

Costa, M., Sweeton, D. and Wieschaus, E. (1993). Gastrulation in Drosophila: Cellular mechanisms of morphogenetic movements. In *The Development of Drosophila melanogaster* (ed. M. Bate and A. Martinez Arias) Cold Spring Harbor, NY: Cold Spring Harbor Laboratory Press.

Courey, A. J. and Tjian, R. (1988). Analysis of Sp1 in vivo reveals multiple transcriptional domains, including a novel glutamine-rich activation motif. *Cell* **55**, 887-898.

Davis, I. and Ish-Horowicz, D. (1991). Apical localization of pair-rule transcripts requires 3′ sequences and limits protein diffusion in the *Drosophila* blastoderm embryo. *Cell* **67**, 927–940.

Dickson, B. J., Sprenger, F., Morrison, D. and Hafen, E. (1992). Raf functions downstream of Ras1 in the Sevenless signal transduction pathway. *Nature* **360**, 600-603.

Dickson, B. J., Dominguez, M., van der Straten, A. and Hafen, E. (1995).

Control of *Drosophila* photoreceptor cell fates by Phyllopod, a novel nuclear protein acting downstream of the Raf kinase *Cell* **80**, 453.

Dickson, B. J., van der Straten, A., Dominguez, M. and Hafen, E. (1996). Mutations Modulating Raf signaling in *Drosophila* eye development. *Genetics* **142**, 163-171.

DiNardo, S. and O'Farrell, P. (1987). Establishment and refinement of segmental pattern in the *Drosophila* embryo. spatial control of engrailed expression by pair-rule genes. *Genes Dev.* **1**, 1212-1225.

Duffy, J. B. and Perrimon, N. (1994). The torso pathway in *Drosophila*: lessons on receptor tyrosine kinase signaling and pattern formation. *Dev. Biol.* **166**, 380-395.

Edgar, B. A. (1999). From small flies come big discoveries about size control. *Nature Cell Biol.* **1**, E191-193.

Fan, S. S. and Ready. D. F. (1997). Glued participates in distinct microtubule-based activities in *Drosophila* eye development. *Development* **124**, 1497-1507.

Feig, L. A. and Cooper, G. M. (1988). Relationship among guanine nucleotide exchange, GTP hydrolysis, and transforming potential of mutated ras proteins. *Mol. Cell. Biol.* **8**, 2472-2478.

Fischer-Vize, J. A. and Mosley, K. L. (1994). Marbles mutants: uncoupling cell determination and nuclear migration in the developing *Drosophila* eye. *Development* **120**, 2609-2618.

Foe, V. F., Odell, G. M. and Edgar, B. A. (1993). Mitosis and morphogenesis in the *Drosophila* embryo: point and counterpoint. In *The Development of Drosophila melanogaster* (ed. M. Bate and A. Martinez Arias) Cold Spring Harbor, NY: Cold Spring Harbor Laboratories Press.

Fortini, M. E., Simon, M. A. and Rubin, G. M. (1992). Signalling by the *sevenless* protein tyrosine kinase is mimicked by Ras1 activation. *Nature* **355**, 559-561.

Gao, X., Neufeld, T. P. and Pan, D. (2000). *Drosophila* PTEN regulates cell growth and proliferation through PI3K-dependent and −independent pathways. *Dev. Biol.* **221**, 404-418.

Gecz, J., Gedeon, A. K., Sutherland, G. R. and Mulley, J. C. (1996). Identification of the gene FMR2, associated with FRAXE mental retardation. *Nature Genet.* **13**, 105-108.

Gecz, J., Bielby, S., Sutherland, G. R. and Mulley, J. C. (1997). Gene structure and subcellular localization of FMR2, a member of a new family of putative transcription activators. *Genomics* **44**, 201-213.

Goberdhan, D. C., Paricio, N., Goodman, E. C., Mlodzik, M. and Wilson, C. (1999). *Drosophila* tumor suppressor PTEN controls cell size and number by antagonizing the Chico/PI3-kinase signaling pathway. *Genes Dev.* **13**, 3244-3258.

Greenwood, S. and Struhl, G. (1997). Different levels of Ras activity can specify distinct transcriptional and morphological consequences in early *Drosophila* embryos. *Development* **124**, 4879-4886.

Gross, S. P., Welte, M. A., Block, S. M. and Wieschaus, E. (2000). Dynein-mediated cargo transport in vivo. A switch controls travel distance. *J. Cell Biol.* **148**, 945-956.

Grosschedl, R., Giese, K. and Pagel, J. (1994). HMG domain proteins: architectural elements in the assembly of nucleoprotein structures. *Trends Genet.* **10**, 94-100.

Gu, Y., Nakamura, T., Alder, H., Prasad, R., Canaani, O., Cimino, G., Croce, C. M. and Canaani, E. (1992). The t(4;11) chromosome translocation of human acute leukemias fuses the ALL-1 gene, related to Drosophila trithorax, to the AF-4 gene. *Cell* **71**, 701-8.

Gu Y., Shen, Y., Gibbs, R.A. and Nelson, D. L. (1996). Identification of FMR2, a novel gene associated with the FRAXE CCG repeat and CpG island. *Nature Genet.* **13**, 109-113.

Guichet, A., Copeland, J. W. R., Erdelyi, M., Hlousek, D., Zavorsky, P., Ho., J., Brown, S., Percival-Smith, A., Krause, H. M. and Ephrussi, A. (1997). The nuclear receptor homologue Ftz-F1 and the homeodomain protein Ftz are mutually dependent cofactors. *Nature* **385**, 548-552.

Hafen, E., Kuroiwa, A. and Gehring, W. J. (1984). Spatial distribution of transcripts from the segmentation gene *fushi tarazu* during *Drosophila* embryonic development. *Cell* **37**, 833–841.

Hay, B. A., Wolff, T. and Rubin, G. M. (1994). Expression of baculovirus p35 prevents cell death in *Drosophila. Development* **120**, 2121-2129.

Huang, H., Potter, C. J., Tao, W., Li, D. M., Brogiolo, W., Hafen, E., Sun, H. and Xu, T. (1999). PTEN affects cell size, cell proliferation and apoptosis during *Drosophila* eye development. *Development* **126**, 5365-72.

Hunter, C. and Wieschaus, E. (2000). Regulated expression of *nullo* is required for the formation of distinct apical and basal adherens junctions in the *Drosophila* blastoderm. *J. Cell Biol.* **150**, 391-401.

Ibnsouda, S., Schweisguth, F., de Billy, G. and Vincent, A. (1993). Relationship between expression of serendipity α and cellularization of the *Drosophila* embryo as revealed by interspecies transformation. *Development* **119**, 471-483.

Ibnsouda, S., Schweisguth, F., Jullien, D., Kücherer, C., Lepesant, J.-A. and Vincent, A. (1995). Evolutionarily conserved positive and negative cis-acting elements control the blastoderm-specific expression of the Drosophila serendipity a cellularization gene. *Mech. Dev.* **49**, 71-82.

Ingham, P. W. and Martinez Arias, A. (1992). Boundaries and fields in early embryos. *Cell* **68**, 221-235.

Ingham, P. W., Howard, K. R. and Ish-Horowicz, D. (1985). Transcription pattern of the *Drosophila* segmentation gene *hairy*. *Nature* **318**, 439–445.

Irvine, K. D. and Wieschaus, E. (1994). Cell intercalation during *Drosophila* germband extension and its regulation by pair-rule segmentation genes. *Development* **120**, 827-841.

Kimmel, B. E., Heberlein, U. and Rubin, G. M. (1990). The homeodomain protein rough is expressed in a subset of cells in the developing *Drosophila* eye where it can specify photoreceptor cell subtype. *Genes Dev.* **4**, 712-727.

Lall, S., Francis-Lang, H., Flament, A., Norvell, A., Schupbach, T. and Ish-Horowicz, D. (1999). Squid hnRNP protein promotes apical cytoplasmic transport and localization of *Drosophila* pair-rule transcripts. *Cell* **98**, 171-180.

Lehner, C. F. (1999). The beauty of small flies. *Nature Cell Biol.* **1**, E129-30.

Lu, X., Perkins, L. A. and Perrimon, N. (1993). The torso signaling pathway in *Drosophila*: a model system to study receptor tyrosine signal transduction. *Development* **Supplement** 47-56.

Ma, C. and Staudt, L. M. (1996). LAF-4 encodes a lymphoid nuclear protein with transactivation potential that is homologous to AF-4, the gene fused to MLL in t(4;11) leukemias. *Blood* **87**, 734-45.

McGhee, J. D. and Felsenfeld, G. (1980). Nucleosome structure. *Annu. Rev. Biochem.* **49**, 1115-1156.

Melnick, M. B., Perkins, L. A., Lee, M., Ambrosio, L. and Perrimon, N. (1993). Developmental and molecular characterization of mutations in the *Drosophila*-raf serine/threonine protein kinase. *Development* **118**, 127-138.

Merrill, P. T., Sweeton, D. and Wieschaus, E. (1988). Requirements for autosomal gene activity during precellular stages of *Drosophila melanogaster*. *Development* **104**, 495-509.

Montagne J., Stewart, M. J., Stocker, H., Hafen, E., Kozma, S. C. and Thomas, G. (1999). *Drosophila* S6 kinase: a regulator of cell size. *Science* **285**, 2126-2129.

Müller, H. A. J. and Wieschaus, E. (1996). *armadillo*, *bazooka*, and *stardus*t are critical for early stages in formation of the zonula adherens and maintenance of the polarized blastoderm epithelium in *Drosophila*. *J. Cell Biol.* **134**, 149-163.

Müller, H. A. J., Samanta, R. and Wieschaus, E. (1999). Wingless signaling in *Drosophila*: zygotic requirements and the role of the frizzled genes. *Development* **126**, 577-586.

Neufeld, T. P., de la Cruz, A. F., Johnston, L. A. and Edgar, B. A. (1998a). Coordination of growth and cell division in the *Drosophila* wing. *Cell* **93**, 1183-1193.

Neufeld, T. P., Tang, A. H. and Rubin, G. M. (1998b). A genetic screen to identify components of the sina signaling pathway in *Drosophila* eye development. *Genetics* **148**, 277-286.

Nüsslein-Volhart, C. and Wieschaus, E. (1980). Mutations affecting segment number and polarity in Drosophila. *Nature* **287**, 795-801.

O'Neill, E. M., Ellis, M. C., Rubin, G. M. and Tjian, R. (1995). Functional domain analysis of glass, a zinc-finger-containing transcription factor in *Drosophila*. *Proc. Natl. Acad. Sci. USA* **92**, 6557-61.

Perrimon N., Lanjuin, A., Arnold, C. and Noll, E. (1996). Zygotic lethal mutations with maternal effect phenotypes in *Drosophila melanogaster.* II. Loci on the second and third chromosomes identified by P-element-induced mutations. *Genetics* **144**, 1681-1692.

Postner, M. and Wieschaus, E. (1994). The nullo protein is a component of the actin-myosin network that mediates cellularization in *Drosophila melanogaster* embryos. *J. Cell Sci.* **107**, 1863-1873.

Rebay, I., Chen, F., Hsiao, F., Kolodziej, P. A. Kuang, B. H., Laverty, T., Suh, C., Voas, M., Williams, A. and Rubin, G. M. (2000). A genetic screen for novel components of the Ras/Mitogen-activated protein kinase signaling pathway that interact with the *yan* gene of *Drosophila* identifies split ends, a new RNA recognition motif-containing protein. *Genetics* **154**, 695-712.

Reeves, R. and Nissen, M. S. (1990). The A.T-DNA-binding domain of mammalian high mobility group I chromosomal proteins. A novel peptide motif for recognizing DNA structure. *J. Biol. Chem.* **265**, 8573-8582.

Reuter, R. and Leptin, M. (1994). Interacting functions of *snail*, *twist* and *huckebein* during the early development of germ layers in *Drosophila*. *Development* **120**, 1137-1150.

Rubin, G. M., Hong, L., Brokstein, P., Evans-Holm, M., Frise, E., Stapleton, M. and Harvey, D. A. (2000). A *Drosophila* complementary DNA resource. *Science* **287**, 2222-2224.

Schejter, E. and Wieschaus, E. (1993a). Functional elements of the cytoskeleton in the early *Drosophila* embryo. *Ann. Rev. Cell Biol.* **9**, 67-99.

Schejter, E. and Wieschaus, E. (1993b). bottleneck acts as a regulator of the microfilament network governing cellularization of the *Drosophila* embryo. *Cell* **75**, 373-385.

Schweisguth, F., Yanicostas, C., Payre, F., Lepesant, J.-A. and Vincent, A. (1989). cis-regulatory elements of the *Drosophila* blastoderm-specific *serendipity* α gene: ectopic acitivation in the embryonic PNS promoted by the deletion of an upstream region. *Dev. Biol.* **136**, 181-193.

Schweisguth, F., Lepesant, J.-A. and Vincent, A. (1990). The serendipity alpha gene encodes a membrane-associated protein required for the cellularization of the *Drosophila* embryo. *Gen. Dev*. **4**, 922-931.

Simpson, L. and Wieschaus, E. (1990). Zygotic activity of the nullo locus is required to stabilize the actin-myosin network during cellularization in *Drosophila*. *Development* **110**, 851-863.

Simpson-Rose, L. and Wieschaus, E. (1992). The *Drosophila* cellularization gene nullo produces a blastoderm specific transcript whose level respond to the nucleocytoplasmic ratio. *Gen. Dev*. **6**, 1235-1268.

St Johnston, D. and Nüsslein-Volhard, C. (1992). The origin of pattern and polarity in the *Drosophila* embryo. *Cell* **68**, 201-219.

Taki, T., Kano, H., Taniwaki, M., Sako, M., Yanagisawa, M. and Hayashi, Y. (1999). AF5q31, a newly identified AF4-related gene, is fused to MLL in infant acute lymphoblastic leukemia with ins(5;11)(q31;q13q23). *Proc. Natl. Acad. Sci. USA* **96**, 14535-40.

Tautz, D. and Pfeifle, C. (1989). A non-radioactive in situ hybridization protocol for the localization of specific transcripts in *Drosophila* embryos reveals transcriptional control of the segmentation gene hunchback. *Chromosoma* **98**, 81-89.

Verdu, J., Buratovich, M. A., Wilder, E. L. and Birnbaum, M. J. (1999). Cell-autonomous regulation of cell and organ growth in *Drosophila* by Akt/PKB. *Nature Cell Biol.* **1**, 500-506.

Wang, S. L., Hawkins, C. J., Yoo, S. J., Müller, H. A. J. and Hay, B. A. (1999). The *Drosophila* caspase inhibitor DIAP1 is essential for cell survival and is negatively regulated by HID. *Cell* **98**, 453-463.

Weinkove, D., Neufeld, T. P., Twardzik, T., Waterfield, M. D. and Leevers, S. J. (1999). Regulation of imaginal disc cell size, cell number and organ size by *Drosophila* class I(A) phosphoinositide 3-kinase and its adaptor. *Curr. Biol.* **9**, 1019-1029.

Weinkove, D. and Leevers, S. J. (2000). The genetic control of organ growth: insights from *Drosophila*. *Curr. Opin. Genet. Dev.* **10**, 75-80.

Welte, M., Gross, S., Postner, M., Block, S. M. and Wieschaus, E. (1998). Developmental regulation of vesicle transport in *Drosophila* embryos: Forces and kinetics. *Cell* **92**, 547-557.

Wieschaus, E. and Sweeton, D. (1988). Requirements for X-linked zygotic activity during cellularization of early *Drosophila* embryos. *Development* **104**, 483-493.

Wolff, T. and Ready, D. F. (1991). Cell death in normal and rough eye mutants of *Drosophila*. *Development* **113**, 825-839.

Xu, T. and Rubin, G.M. (1993). Analysis of genetic mosaics in developing and adult *Drosophila* tissues. *Development* **117**, 1223-1237.

Yu, Y., Li, W., Su, K., Yussa, M., Han, W., Perrimon, N. and Pick, L. (1997). The nuclear hormone receptor Ftz-F1 is a cofactor of the *Drosophila* homeodomain protein Ftz. *Nature* **385**, 552-555.

Zhang H., Stallock, J. P., Ng, J. C., Reinhard, C. and Neufeld, T. P. (2000). Regulation of cellular growth by the *Drosophila* target of rapamycin, *dTOR*. *Genes Dev.* **14**, 2712-2724.